

# Matrix Sketching for Secure Collaborative Machine Learning

Shusen Wang and Mengjiao Zhang

Department of Computer Science

Stevens Institute of Technology

Hoboken, NJ 07030

{shusen.wang, mzhang49}@stevens.edu

## Abstract

Collaborative learning allows participants to jointly train a model without data sharing. To update the model parameters, the central server broadcasts model parameters to the clients, and the clients send updating directions such as gradients to the server. While data do not leave a client device, the communicated gradients and parameters will leak a client’s privacy. Prior work proposed attacks that infer client’s privacy from gradients and parameters. They also showed that simple defenses such as dropout and differential privacy do not help much.

We propose a practical defense which we call Double Blind Collaborative Learning (DBCL). The high-level idea is to apply random matrix sketching to the parameters (aka weights) and re-generate random sketching after each iteration. DBCL prevents malicious clients from conducting gradient-based privacy inference which are the most effective attacks. DBCL works because from the attacker’s perspective, sketching is effectively random noise that outweighs the signal. Notably, DBCL does not increase the computation and communication cost much and does not hurt test accuracy at all.

## 1 Introduction

Collaborative learning allows multiple parties to jointly train a model using their private data but without sharing the data. Collaborative learning is motivated by real-world applications, for example, training a model using but without collecting mobile user’s data.

Distributed stochastic gradient descent (SGD), as illustrated in Figure 1, is perhaps the simplest approach to collaborative learning. Specifically, the central server broadcasts model parameters to the clients, each client uses a batch of local data to evaluate a stochastic gradient, and the server aggregates the stochastic gradients and updates the model parameters. Based on distributed SGD, communication-efficient algorithms such as federated averaging (FedAvg) [32] and FedProx [39] have been developed and analyzed [26, 43, 48, 52, 57].

Collaboratively learning seemingly protects clients’ privacy. Unfortunately, it has been demonstrated not true by recent studies [19, 33, 58]. Even if a client’s data do not leave his device, important properties of his data can be disclosed from the model parameters and gradients. To infer other clients’ data, the attacker needs only to control one client device and access the model parameters in every iteration; the attacker does not have to take control of the server [19, 33, 58].

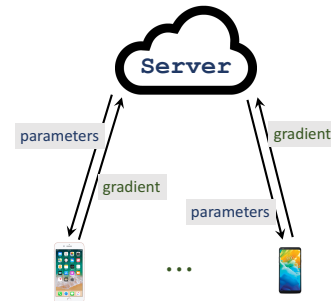


Figure 1: Collaborative learning with a central parameter server

The reason why the attacks work is that model parameters and gradients carry important information about the training data [2, 14]. In [19], the jointly learned model is used as a discriminator for training a generator which generates other clients’ data. In [33], gradient is used for inferring other clients’ data properties. In [58], model parameters and gradients are both used for reproducing other clients’ data. Judging from published empirical studies, the gradient-based attacks [33, 58] are more effective than the parameter-based attack [19]. Our goal is to defend the gradient-based attacks.

Simple defenses, e.g., differential privacy [12] and dropout [42], have been demonstrated not working well by [19, 33]. While differential privacy [12], i.e., adding noise to model parameters or gradients, works if the noise is strong, the noise evitably hurts the accuracy and may even stop the collaborative learning from making progress [19]. If the noise is not strong enough, clients’ privacy will leak. Dropout training [42] randomly masks a fraction of the parameters, making the clients have access to only part of the parameters in each iteration. However, knowing part of the parameters is sufficient for conducting the attacks.

## 1.1 Our Contributions and Limitations

We propose *Double-Blind Collaborative Learning (DBCL)* as a practical defense against gradient-based attacks, e.g., [33, 58]. Using DBCL, one client cannot make use of gradients to infer other clients’ privacy. DBCL applies random sketching to every or some layers of a neural network, and the random sketching matrices are regenerated after each iteration. Throughout the training, the clients do not see the real model parameters, and the server does not see any real gradient or descending direction. This is why we call our method *double-blind*.

DBCL has the following nice properties. First, DBCL does not hinder test accuracy at all. Second, DBCL does not increase the per-iteration time complexity and communication complexity, although it reasonably increases the iterations for attaining convergence. Last but not least, to apply DBCL to dense layers and convolutional layers, no additional tuning is needed.

While we propose DBCL as a practical defense against gradient-based attacks at little cost, we do not claim DBCL as a panacea. DBCL has two limitations. First, with DBCL applied, a malicious client cannot perform gradient-based attacks, but he may be able to perform parameter-based attacks such as [19]; fortunately, the latter is much less effective than the former. Second, DBCL cannot prevent a malicious server from inferring clients’ privacy, although DBCL makes the server’s attack much less effective.

In sum, DBCL can defend gradient-based attacks conducted by a client and make other types of attacks less effective. We admit that DBCL alone does not fundamentally defend all the attacks. To the best of our knowledge, there does not exist any defense that is effective for all the attacks that infer privacy. DBCL can be easily incorporated with existing methods such as homomorphic encryption and secret sharing to defend more attacks.

## 1.2 Paper Organization

Section 2 introduces neural network, backpropagation, and matrix sketching. Section 3 defines threat models. Section 4 describes the algorithm, including the computation and communication. Section 5 presents empirical results to demonstrate that DBCL does not harm test accuracy, does not much increase the communication cost, and can defend gradient-based attacks. Section 6 theoretically studies DBCL. Section 7 discusses some closely relevant work. Algorithm derivations and theoretical proofs are in the appendix. The source code is available at the Github repo: <https://github.com/MengjiaoZhang/DBCL.git>

## 2 Preliminaries

**Dense layer.** Let  $d_{in}$  be the input shape,  $d_{out}$  be the output shape, and  $b$  be the batch size. Let  $\mathbf{X} \in \mathbb{R}^{b \times d_{in}}$  be the input,  $\mathbf{W} \in \mathbb{R}^{d_{out} \times d_{in}}$  be the parameter matrix, and  $\mathbf{Z} = \mathbf{X}\mathbf{W}^T$  be the output. After the dense (aka fully-connected) layer, there is typically an activation function  $\sigma(\mathbf{Z})$  applied elementwisely.

**Backpropagation.** Let  $L$  be the loss evaluated on a batch of  $b$  training samples. We derive backpropagation for the dense layer by following the convention of PyTorch. Let  $\mathbf{G} \triangleq \frac{\partial L}{\partial \mathbf{Z}} \in \mathbb{R}^{b \times d_{out}}$  be the gradient received from the upper layer. We need to compute the gradients:

$$\frac{\partial L}{\partial \mathbf{X}} = \mathbf{G}\mathbf{W} \in \mathbb{R}^{b \times d_{in}} \quad \text{and} \quad \frac{\partial L}{\partial \mathbf{W}} = \mathbf{G}^T \mathbf{X} \in \mathbb{R}^{d_{out} \times d_{in}},$$

which can be established by the chain rule. We use  $\frac{\partial L}{\partial \mathbf{W}}$  to update the parameter matrix  $\mathbf{W}$  by e.g.,  $\mathbf{W} \leftarrow \mathbf{W} - \eta \frac{\partial L}{\partial \mathbf{W}}$ , and pass  $\frac{\partial L}{\partial \mathbf{X}}$  to the lower layer.

**Uniform sampling matrix.** We call  $\mathbf{S} \in \mathbb{R}^{d_{in} \times s}$  a uniform sampling matrix if its columns are sampled from the set  $\{\frac{\sqrt{d_{in}}}{\sqrt{s}} \mathbf{e}_1, \dots, \frac{\sqrt{d_{in}}}{\sqrt{s}} \mathbf{e}_{d_{in}}\}$  uniformly at random. Here,  $\mathbf{e}_i$  is the  $i$ -th standard basis of  $\mathbb{R}^{d_{in}}$ . We call  $\mathbf{S}$  a uniform sampling matrix because  $\mathbf{X}\mathbf{S}$  contains  $s$  randomly sampled (and scaled) columns of  $\mathbf{X}$ . Random matrix theories [10, 30, 31, 51] guarantee that  $\mathbb{E}_{\mathbf{S}}[\mathbf{X}\mathbf{S}\mathbf{S}^T \mathbf{W}^T] = \mathbf{X}\mathbf{W}$  and that  $\|\mathbf{X}\mathbf{S}\mathbf{S}^T \mathbf{W}^T - \mathbf{X}\mathbf{W}\|$  is bounded, for any  $\mathbf{X}$  and  $\mathbf{W}$ .

**CountSketch.** We call  $\mathbf{S} \in \mathbb{R}^{d_{in} \times s}$  a CountSketch matrix [6, 8, 36, 45, 50] if it is constructed in the following way. Every row of  $\mathbf{S}$  has exactly one nonzero entry whose position is randomly sampled from  $[s] \triangleq \{1, 2, \dots, s\}$  and value is sampled from  $\{-1, +1\}$ . Here is an example of  $\mathbf{S}$  ( $10 \times 3$ ):

$$\mathbf{S}^T = \begin{bmatrix} 0 & 0 & 1 & -1 & 1 & -1 & 0 & 0 & 0 & 0 \\ -1 & 0 & 0 & 0 & 0 & 0 & 0 & 1 & 1 & -1 \\ 0 & -1 & 0 & 0 & 0 & 0 & 0 & 0 & 0 & 1 \end{bmatrix}.$$

CountSketch has very similar properties as random Gaussian matrices [20, 51]. We use CountSketch for its computation efficiency. Given  $\mathbf{X} \in \mathbb{R}^{b \times d_{in}}$ , the CountSketch  $\tilde{\mathbf{X}} = \mathbf{X}\mathbf{S}$  can be computed in  $\mathcal{O}(d_{in}b)$  time. CountSketch is much faster than the standard matrix multiplication which has  $\mathcal{O}(d_{in}bs)$  time complexity. Theories in [8, 34, 35, 51] guarantee that  $\mathbb{E}_{\mathbf{S}}[\mathbf{X}\mathbf{S}\mathbf{S}^T \mathbf{W}^T] = \mathbf{X}\mathbf{W}$  and that  $\|\mathbf{X}\mathbf{S}\mathbf{S}^T \mathbf{W}^T - \mathbf{X}\mathbf{W}\|$  is bounded, for any  $\mathbf{X}$  and  $\mathbf{W}$ . In practice,  $\mathbf{S}$  is never explicitly constructed.

### 3 Threat Models

In this paper, we consider the attacks and defenses under the setting of client-server architecture and assume the attacker controls a client.<sup>1</sup> Let  $\mathbf{W}_{old}$  and  $\mathbf{W}_{new}$  be the model parameters (aka weights) in two consecutive iterations. The server broadcasts  $\mathbf{W}_{old}$  to the clients, the  $m$  clients use  $\mathbf{W}_{old}$  and their local data to compute ascending directions  $\Delta_1, \dots, \Delta_m$  (e.g., gradients), and the server aggregates the directions by  $\Delta = \frac{1}{m} \sum_{i=1}^m \Delta_i$  and performs the update  $\mathbf{W}_{new} \leftarrow \mathbf{W}_{old} - \Delta$ . Since a client (say the  $k$ -th) knows  $\mathbf{W}_{old}$ ,  $\mathbf{W}_{new}$ , and his own direction  $\Delta_k$ , he can calculate the sum of other clients' directions by

$$\sum_{i \neq k} \Delta_i = m\Delta - \Delta_k = m(\mathbf{W}_{old} - \mathbf{W}_{new}) - \Delta_k. \quad (1)$$

In the case of two-party collaborative learning, that is,  $m = 2$ , one client knows the updating direction of the other client.

Knowing the model parameters, gradients, or both, the attacker can use various ways [19, 33, 58] to infer other clients' privacy. We focus on gradient-based attacks [33, 58], that is, the victim's privacy is extracted from the gradients. Melis *et al.* (2019) [33] built a classifier and locally trained it for property inference. The classifier takes the updating direction  $\Delta_i$  as input feature and predicts the clients' data properties. The client's data cannot be recovered, however, the classifier can tell, e.g., the photo is likely female. Zhu *et al.* (2019) [58] developed an optimization method called *gradient matching* for recovering other clients' data; both gradient and model parameters are used. It has been shown that simple defenses such as differential privacy [13, 12] and dropout [41] cannot defend the attacks.

In decentralized learning, where participants are compute nodes in a peer-to-peer network, a node knows its neighbors' model parameters and thus updating directions. A malicious node can infer the privacy of its neighbors in the same way as [33, 58]. In Appendix C, we discuss the attack and defense in decentralized learning; they will be our future work.

### 4 Proposed Method: Double-Blind Collaborative Learning (DBCL)

We present the high-level ideas in Section 4.1, elaborate on the implementation in Section 4.2, and analyze the time and communication complexities in Section 4.3.

<sup>1</sup>A stronger assumption would be that the server is malicious. Our defense may not defeat a malicious server.

## 4.1 High-Level Ideas

The attacks of [33, 58] need the victim’s updating direction, e.g., gradient, for inferring the victim’s privacy. Using standard distributed algorithms such as distributed SGD and Federated Averaging (FedAvg) [32], the server can see the clients’ updating directions,  $\Delta_1, \dots, \Delta_m$ , and the clients can see the jointly learned model parameter,  $\mathbf{W}$ . A malicious client can use (1) to get other clients’ updating directions and then perform the gradient-based attacks such as [33, 58].

To defend the gradient-based attacks, our proposed Double-Blind Collaborative Learning (DBCL) applies random sketching to the parameter matrices and regenerate random sketching after each iteration. From the normal clients’ perspective, the sketching is similar to dropout regularization which does not hurt accuracy; see Section 6.3. From the malicious client’s perspective, the sketching is effectively random noise that outweighs “signal” in the gradient; see (3).

To be more specific, only the server knows the true model parameters,  $\mathbf{W}$ . What the server broadcasts to the clients are random sketches of  $\mathbf{W}$ , and the sketching matrix varies after each iteration. Let  $\mathbf{W}_{\text{old}}$  and  $\mathbf{W}_{\text{new}}$  be the true model parameters in two consecutive iterations; they are known to only the server. What the clients observe are the random sketches:  $\widetilde{\mathbf{W}}_{\text{old}} = \mathbf{W}_{\text{old}}\mathbf{S}_{\text{old}}$  and  $\widetilde{\mathbf{W}}_{\text{new}} = \mathbf{W}_{\text{new}}\mathbf{S}_{\text{new}}$ .

We explain why we use random projection rather than random sampling. The attacker (a malicious client) needs to know the gradient  $\Delta = \mathbf{W}_{\text{old}} - \mathbf{W}_{\text{new}}$  (approximately) in order to conduct any gradient-based attack. With  $s = 0.5d_{\text{in}}$ , which is the typical setting of dropout training, uniform sampling randomly masks 50% of the columns of  $\mathbf{W}_{\text{old}}$  and  $\mathbf{W}_{\text{new}}$ . Unfortunately, even with the random mask, the attacker still knows 25% of the columns of  $\Delta$  and can perform the attack, although less effectively. If  $\mathbf{S}$  is random projection such as CountSketch [51] or random Gaussian matrix [20], the attacker’s observation of  $\Delta$  is very noisy; see Section 6.

## 4.2 Algorithm Description

We describe the computation and communication operations of DBCL. We consider the client-server architecture, dense layers, and the distributed SGD algorithm.<sup>2</sup> DBCL works in the following four steps. Broadcasting and aggregation are communication operations; forward pass and backward pass are local computations performed by each client for calculating gradients.

**Broadcasting.** The central server generates a new seed  $\psi^3$  and then a random sketch:  $\widetilde{\mathbf{W}} = \mathbf{W}\mathbf{S}$ . It broadcasts  $\psi$  and  $\widetilde{\mathbf{W}} \in \mathbb{R}^{d_{\text{out}} \times s}$  to all the clients through message passing. Here, the sketch size  $s$  is determined by the server and must be set smaller than  $d_{\text{in}}$ ; the server can vary  $s$  after each iteration.

**Local forward pass.** The  $i$ -th client randomly selects a batch of  $b$  samples from its local dataset and then locally performs a forward pass. Let the input of a dense layer be  $\mathbf{X}_i \in \mathbb{R}^{b \times d_{\text{in}}}$ . The client uses the seed  $\psi$  to draw a sketch  $\widetilde{\mathbf{X}}_i = \mathbf{X}_i\mathbf{S} \in \mathbb{R}^{b \times s}$  and computes  $\mathbf{Z}_i = \widetilde{\mathbf{X}}_i\widetilde{\mathbf{W}}^T$ . Then  $\sigma(\mathbf{Z}_i)$  becomes the input of the upper layer, where  $\sigma$  is some activation function. Repeat this process for all the layers. The forward pass finally outputs  $L_i$ , the loss evaluated on the batch of  $b$  samples.

**Local backward pass.** Let the local gradient propagated to the dense layer be  $\mathbf{G}_i \triangleq \frac{\partial L_i}{\partial \mathbf{Z}_i} \in \mathbb{R}^{b \times d_{\text{out}}}$ . The client locally calculates

$$\mathbf{\Gamma}_i = \mathbf{G}_i^T \widetilde{\mathbf{X}}_i \in \mathbb{R}^{d_{\text{out}} \times s} \quad \text{and} \quad \frac{\partial L_i}{\partial \mathbf{X}_i} = \mathbf{G}_i \widetilde{\mathbf{W}}\mathbf{S}^T \in \mathbb{R}^{b \times d_{\text{in}}}.$$

The gradient  $\frac{\partial L_i}{\partial \mathbf{X}_i}$  is propagated to the lower-level layer to continue the backpropagation.

**Aggregation.** The server aggregates  $\{\mathbf{\Gamma}_i\}_{i=1}^m$  to compute  $\mathbf{\Gamma} = \frac{1}{m} \sum_{i=1}^m \mathbf{\Gamma}_i$ ; this needs a communication. Let  $L = \frac{1}{m} \sum_{i=1}^m L_i$  be the loss evaluated on the batch of  $mb$  samples. It can be shown that

$$\frac{\partial L}{\partial \mathbf{W}} = \frac{1}{m} \sum_{i=1}^m \frac{\partial L_i}{\partial \mathbf{W}} = \mathbf{\Gamma}\mathbf{S}^T \in \mathbb{R}^{d_{\text{out}} \times d_{\text{in}}}. \quad (2)$$

The server then updates the parameters by, e.g.,  $\mathbf{W} \leftarrow \mathbf{W} - \eta \frac{\partial L}{\partial \mathbf{W}}$ .

<sup>2</sup>DBCL works also for convolutional layers; see Appendix A.2 for the details. DBCL can be easily extended to FedAvg or other communication-efficient frameworks. DBCL can be applied to peer-to-peer networks; see the discussions in Appendix C.

<sup>3</sup>Let the clients use the same pseudo-random number generator as the server. Given the seed  $\psi$ , all the clients can construct the same sketching matrix  $\mathbf{S}$ .

### 4.3 Time Complexity and Communication Complexity

DBCL does not increase the time complexity of local computations. The CountSketch,  $\tilde{\mathbf{X}}_i = \mathbf{X}_i \mathbf{S}$  and  $\tilde{\mathbf{W}}_i = \mathbf{W}_i \mathbf{S}$ , costs  $\mathcal{O}(bd_{in})$  and  $\mathcal{O}(d_{in}d_{out})$  time, respectively. Using CountSketch, the overall time complexity of a forward and a backward pass is  $\mathcal{O}(bd_{in} + d_{in}d_{out} + bsd_{out})$ . Since we set  $s < d_{in}$  to protect privacy, the time complexity is lower than the standard backpropagation,  $\mathcal{O}(bd_{in}d_{out})$ .

DBCL does not increase per-iteration communication complexity. Without using sketching, the communicated matrices are  $\mathbf{W} \in \mathbb{R}^{d_{out} \times d_{in}}$  and  $\frac{\partial L_i}{\partial \mathbf{W}} \in \mathbb{R}^{d_{out} \times d_{in}}$ . Using sketching, the communicated matrices are  $\tilde{\mathbf{W}} \in \mathbb{R}^{d_{out} \times s}$  and  $\tilde{\Gamma}_i \in \mathbb{R}^{d_{out} \times s}$ . Because  $s < d_{in}$ , the per-iteration communication complexity is lower than the standard distributed SGD.

## 5 Experiments

We conduct experiments to demonstrate that first, DBCL does not harm test accuracy, second, DBCL does not increase the communication cost too much, and third, DBCL can defend the gradient-based attacks of [33, 58].

### 5.1 Experiment Setting

Our method and the compared methods are implemented using PyTorch. The experiments are conducted on a server with 4 NVIDIA GeForce Titan V GPUs, 2 Xeon Gold 6134 CPUs, and 192 GB memory. We follow the settings of the relevant papers to perform comparisons.

Three datasets are used in the experiments. MNIST has 60,000 training images and 10,000 test images; each image is  $28 \times 28$ . CIFAR-10 has 50,000 training images and 10,000 test images; each image is  $32 \times 32 \times 3$ . Labeled Faces In the Wild (LFW) has 13,233 faces of 5,749 individuals; each face is a  $64 \times 47 \times 3$  color image.

### 5.2 Accuracy and Efficiency

We conduct experiments on the MNIST, CIFAR-10, and LFW datasets to show that first, DBCL does not hinder prediction accuracy, and second, it does not much increase the communication cost. The learning rates are tuned to optimize the convergence rate.

**MNIST classification.** We build a multilayer perceptron (MLP) and a convolutional neural network (CNN) for the multi-class classification task. The MLP has 3 dense layers: Dense(200)  $\Rightarrow$  ReLU  $\Rightarrow$  Dense(200)  $\Rightarrow$  ReLU  $\Rightarrow$  Dense(10)  $\Rightarrow$  Softmax. The CNN has 2 convolutional layers and 2 dense layers: Conv(32,  $5 \times 5$ )  $\Rightarrow$  ReLU  $\Rightarrow$  MaxPool( $2 \times 2$ )  $\Rightarrow$  Conv(64,  $5 \times 5$ )  $\Rightarrow$  ReLU  $\Rightarrow$  MaxPool( $2 \times 2$ )  $\Rightarrow$  Flatten  $\Rightarrow$  Dense(512)  $\Rightarrow$  ReLU  $\Rightarrow$  Dense(10)  $\Rightarrow$  Softmax.

We use Federated Averaging (FedAvg) to train the MLP and CNN. We follow the setting of [32]. The data are partitioned among 100 (virtual) clients uniformly at random. Between two communications, FedAvg performs local computation for 1 epoch (for MLP) or 5 epochs (for CNN). The batch size of local SGD is set to 10.

Sketching is applied to all the dense and convolutional layers except the output layer. We set the sketch size  $s = d_{in}/2$ ; thus, the per-iteration communication complexity is reduced by half. With sketching, the MLP and CNN are trained by FedAvg under the same setting.

Table 1: Experiments on MNIST. The table shows the rounds of communications for attaining the test accuracy. Here,  $c$  is the participation ratio of FedAvg, that is, in each round, only a fraction of clients participate in the training..

Models	Accuracy	Communication Rounds				
		$c = 1\%$	$c = 10\%$	$c = 20\%$	$c = 50\%$	$c = 100\%$
MLP	0.97	222	96	84	83	82
MLP-Sketch	0.97	828	429	416	415	408
CNN	0.99	462	309	97	91	31
CNN-Sketch	0.99	344	126	56	46	55

We show the experimental results in Table 1. Trained by FedAvg, the small MLP can only reach 97% validation accuracy, while the CNN can obtain 99% test accuracy. Under all the settings, using sketching does not hinder test accuracy at all. We show the rounds of communications for attaining

the test accuracies. For the MLP, sketching needs 5x communications to converge. For the CNN, sketching does not increase communication cost.

**CIFAR-10 classification.** We build a CNN with 3 convolutional layers and 2 dense layers: Conv(32,  $5 \times 5$ )  $\Rightarrow$  ReLU  $\Rightarrow$  Conv(64,  $5 \times 5$ )  $\Rightarrow$  ReLU  $\Rightarrow$  MaxPool( $2 \times 2$ )  $\Rightarrow$  Conv(128,  $5 \times 5$ )  $\Rightarrow$  ReLU  $\Rightarrow$  MaxPool( $2 \times 2$ )  $\Rightarrow$  Flatten  $\Rightarrow$  Dense(200)  $\Rightarrow$  ReLU  $\Rightarrow$  Dense(10)  $\Rightarrow$  Softmax.

The CNN is also trained using FedAvg. We follow the setting of [32]. The data are partitioned among 100 clients. We set the participation ratio to  $c = 10\%$ , that is, each time only 10% uniformly sampled clients participate in the training. Between two communications, FedAvg performs local computation for 5 epochs. The batch size of local SGD is set to 50. We do not use tricks such as data augmentation.

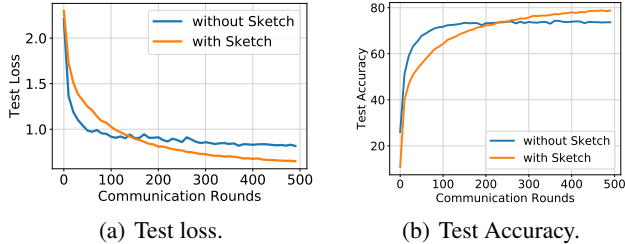


Figure 2: Experiment on CIFAR-10 dataset.

Figure 2 shows the convergence curves. Using sketching does not hinder the validation accuracy at all; on the contrary, it marginally improves the validation accuracy. The reason is likely that sketching is an adaptive regularization similar to dropout [42, 47]; see the discussions in Section 6.3.

**LFW classification (class-imbalanced).** Following [33], we conduct binary classification experiments on a subset of the LFW dataset. We use 8150 faces for training and 3,400 for test. The task is gender prediction. We build a CNN with 3 convolutional layers and 3 dense layers: Conv(64,  $3 \times 3$ )  $\Rightarrow$  ReLU  $\Rightarrow$  MaxPool( $2 \times 2$ )  $\Rightarrow$  Conv(64,  $3 \times 3$ )  $\Rightarrow$  ReLU  $\Rightarrow$  MaxPool( $2 \times 2$ )  $\Rightarrow$  Conv(128,  $3 \times 3$ )  $\Rightarrow$  ReLU  $\Rightarrow$  MaxPool( $2 \times 2$ )  $\Rightarrow$  Flatten  $\Rightarrow$  Dense(32)  $\Rightarrow$  ReLU  $\Rightarrow$  Dense(32)  $\Rightarrow$  ReLU  $\Rightarrow$  Dense(1)  $\Rightarrow$  Sigmoid. We apply sketching to all the convolutional and dense layers except the output layer. The model is trained by distributed SGD (2 clients and 1 server) with a learning rate of 0.01 and a batch size of 32.

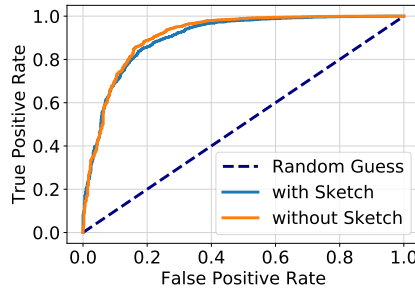


Figure 3: Gender classification on the LFW dataset.

The dataset is class-imbalanced: 8957 are males, and 2593 are females. Using classification accuracy for imbalanced dataset is a bad idea. In Figure 3, we plot the ROC curves to compare the standard CNN and the sketched one. The two ROC curves are almost the same. Using sketching, the true positive rate is marginally worse than the standard CNN.

### 5.3 Defending Gradient-Based Attacks

We empirically study whether DBCL can defend the gradient-based attacks of [33] and [58]. Our setting is two-party ( $m = 2$ ) and distributed SGD algorithm.

**Threat models.** We find that using DBCL, the attack launched by a malicious client does not work at all. Instead, we study a more challenging threat: can DBCL defend a **malicious server**? We assume first, the server is honest but curious, second, the server holds a subset of data, and third, the server knows the true model parameters  $\mathbf{W}$  and the sketched gradients. The assumptions, especially the third, make it easy to attack but hard to defend. Let  $\Gamma_i$  be the sketched gradient of the  $i$ -th client; the server uses  $\Gamma_i \mathbf{S}^T$  to approximate the true gradient; see (2). Throughout, the server uses  $\Gamma_i \mathbf{S}^T$  for privacy inference.

**Defending the property inference attack (PIA) of [33].** We conduct experiments on the LFW dataset by following the settings of [33]. We use one server and two clients. The task of collaborative learning is the gender classification discussed in the LFW experiment in Section 5.2. The collaborative learning settings are the same as Section 5.2. The attacker (malicious server) seeks to infer whether a single batch of photos in the victim’s private dataset contain Africans or not.

The two clients collaboratively train the model on the gender classification task for 20,000 iterations. To conduct the PIA, the malicious server needs a set of data; let the server have the same number of samples as the clients. From the 1,000th to the 20,000th iterations, the server uses the true model parameters and its local dataset to evaluate gradients and use the gradients for training a random forest for the PIA. In each iteration, the attacker uses its auxiliary data to get 2 gradients with property and 8 gradients without property. Thus there are 190,000 gradients for training. We collect one gradient per iteration from the victim for test; there are 19,000 test gradients.

After training the random forest, the malicious server uses it for binary classification. It seeks to infer whether a batch of the victim’s (a client) private images contain Africans or not. The test data are class-imbalanced: only 3,800 gradients are from images of Africans, whereas the rest 15,200 are from non-Africans. We thus use AUC as the evaluation metric. Without sketching, the AUC is 1.0, which means the server can exactly tell whether a batch of client’s images contain Africans or not. Using sketching, the AUC is 0.726. It is much worse than without sketching, which means sketching makes the PIA less effective. Nevertheless, the AUC is better than random guessing (AUC=0.5), which means the PIA is still effective to some extent.

**Defending the gradient matching attack of [58].** Zhu *et al.* [58] proposed to recover the victims’ data using model parameters and gradients. They seek to find a batch of images by optimization so that the resulting gradient matches the observed gradient of the victim. We use the same CNNs as [58] to conduct experiments on the MNIST and CIFAR-10 datasets. We apply sketching to all except the output layer.

In figure 4, we show the recovered images. DBCL successfully defends the gradient-matching attack conducted by the server. What the malicious server knows is the exact model parameters  $\mathbf{W}$ , but the sketching makes the gradients much different. Matching the gradients transformed by sketching cannot produce the original images.

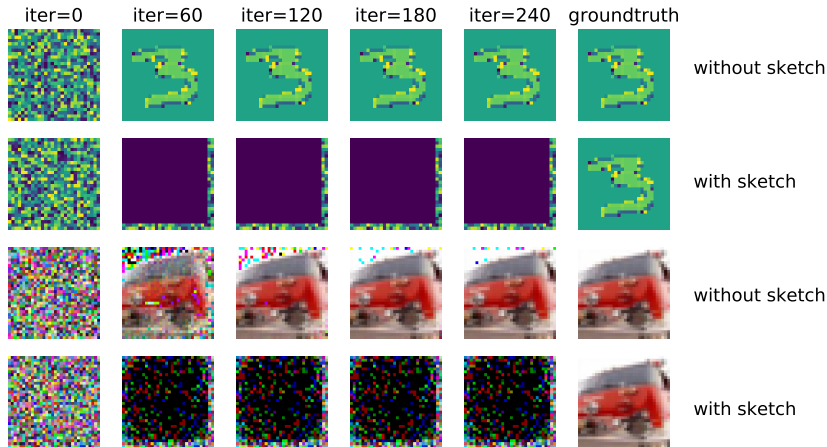


Figure 4: The images are generated by the gradient-matching attack of [58]. The attack is effective for the standard CNNs. Using sketching, the gradient-matching attack cannot recover the images.

## 6 Theoretical Insights

In Section 6.1, we discuss how a malicious client makes use of the sketched model parameters for privacy inference. In Sections 6.2, we show that DBCL can defend certain types of attacks. In Section 6.3, we give an explanation of DBCL from optimization perspective.

### 6.1 Approximating the Gradient

Assume the attacker controls a client and participate in collaborative learning. Let  $\mathbf{W}_{old}$  and  $\mathbf{W}_{new}$  be the parameter matrices of two consecutive iterations; they are unknown to the clients. What a client sees are the sketches,  $\widetilde{\mathbf{W}}_{old} = \mathbf{W}_{old}\mathbf{S}_{old}$  and  $\widetilde{\mathbf{W}}_{new} = \mathbf{W}_{new}\mathbf{S}_{new}$ . To conduct gradient-based attacks, the attacker must know the gradient  $\Delta = \mathbf{W}_{old} - \mathbf{W}_{new}$ .

Naively using  $\widetilde{\mathbf{W}}_{\text{old}}$  and  $\widetilde{\mathbf{W}}_{\text{new}}$  does not work. The difference between sketched parameters,  $\widetilde{\Delta} = \widetilde{\mathbf{W}}_{\text{old}} - \widetilde{\mathbf{W}}_{\text{new}}$ , is entirely different from the real gradient,  $\Delta = \mathbf{W}_{\text{old}} - \mathbf{W}_{\text{new}}$ .<sup>4</sup> We can even vary the sketch size  $s$  with iterations so that  $\widetilde{\mathbf{W}}_{\text{old}}$  and  $\widetilde{\mathbf{W}}_{\text{new}}$  have different number of columns, making it impossible to compute  $\widetilde{\Delta}$ .

Note that the clients know also  $\mathbf{S}_{\text{old}}$  and  $\mathbf{S}_{\text{new}}$ . A smart attacker, who knows random matrix theory, may want to use

$$\widehat{\Delta} = \mathbf{W}_{\text{old}} \mathbf{S}_{\text{old}} \mathbf{S}_{\text{old}}^T - \mathbf{W}_{\text{new}} \mathbf{S}_{\text{new}} \mathbf{S}_{\text{new}}^T$$

to approximate  $\Delta$ , because  $\widehat{\Delta}$  is an unbiased estimate of  $\Delta$ , i.e.,  $\mathbb{E}[\widehat{\Delta}] = \Delta$ , where the expectation is taken w.r.t. the random sketching matrices  $\mathbf{S}_{\text{old}}$  and  $\mathbf{S}_{\text{new}}$ .

## 6.2 Defending Gradient-Based Attacks

We analyze the attack that uses  $\widehat{\Delta}$ . We first give an intuitive explanation and then prove that using  $\widehat{\Delta}$  does not work, unless the magnitude of  $\Delta$  is smaller than  $\mathbf{W}_{\text{new}}$ .

**Matrix sketching as implicit noise.** As  $\widehat{\Delta}$  is an unbiased estimate of  $\Delta$ , the reader may wonder why  $\widehat{\Delta}$  does not disclose the information of  $\Delta$ . We give an intuitive explanation. Note that  $\widehat{\Delta}$  is a mix of  $\Delta$  (which is the signal) and a random transformation of  $\mathbf{W}_{\text{new}}$  (which is random noise):

$$\widehat{\Delta} = \underbrace{\Delta}_{\text{signal}} \mathbf{S}_{\text{old}} \mathbf{S}_{\text{old}}^T + \underbrace{\mathbf{W}_{\text{new}} (\mathbf{S}_{\text{old}} \mathbf{S}_{\text{old}}^T - \mathbf{S}_{\text{new}} \mathbf{S}_{\text{new}}^T)}_{\text{zero-mean noise}}. \quad (3)$$

As the magnitude of  $\mathbf{W}$  is much greater than  $\Delta$ ,<sup>5</sup> the noise outweighs the signal, making  $\widehat{\Delta}$  far from  $\Delta$ . From the attacker's perspective, random sketching is just like random noise which outweighs the signal.

**Defending the property inference attack (PIA) of [33].** To conduct the PIA of [33], the attacker may want to use a linear model parameterized by  $\mathbf{V}$ .<sup>6</sup> According to (1), the attacker uses  $\Delta - \mathbf{A}$  as input features for PIA, where  $\mathbf{A}$  is some fixed matrix known to the attacker. The linear model makes prediction by  $\mathbf{Y} \triangleq (\Delta - \mathbf{A}) \mathbf{V}^T$ . Using  $\widehat{\Delta}$  to approximate  $\Delta$ , the prediction is  $\widehat{\mathbf{Y}} \triangleq (\widehat{\Delta} - \mathbf{A}) \mathbf{V}^T$ . Theorem 1 and Corollary 2 show that  $\|\widehat{\mathbf{Y}} - \mathbf{Y}\|_F^2 = \|\widehat{\Delta} \mathbf{V}^T - \Delta \mathbf{V}^T\|_F^2$  is very big.

**Theorem 1.** *Let  $\mathbf{S}_{\text{old}}$  and  $\mathbf{S}_{\text{new}}$  be  $d_{\text{in}} \times s$  CountSketch matrices and  $s < d_{\text{in}}$ . Let  $w_{pq}$  be the  $(p, q)$ -th entry of  $\mathbf{W}_{\text{old}} \in \mathbb{R}^{d_{\text{out}} \times d_{\text{in}}}$  and  $\tilde{w}_{pq}$  be the  $(p, q)$ -th entry of  $\mathbf{W}_{\text{new}} \in \mathbb{R}^{d_{\text{out}} \times d_{\text{in}}}$ . Let  $\mathbf{V}$  be any  $r \times d_{\text{in}}$  matrix and  $v_{pq}$  be the  $(p, q)$ -th entry of  $\mathbf{V}$ . Then*

$$\mathbb{E} \|\widehat{\Delta} \mathbf{V}^T - \Delta \mathbf{V}^T\|_F^2 = \frac{1}{s} \sum_{i=1}^{d_{\text{out}}} \sum_{j=1}^r \sum_{k \neq l} \left( w_{ik}^2 v_{jl}^2 + w_{ik} v_{jk} w_{il} v_{jl} + \tilde{w}_{ik}^2 v_{jl}^2 + \tilde{w}_{ik} v_{jk} \tilde{w}_{il} v_{jl} \right).$$

The bound in Theorem 1 is involved. To interpret the bound, we add (somehow unrealistic) assumptions and obtain Corollary 2.

**Corollary 2.** *Let  $\mathbf{S}$  be a  $d_{\text{in}} \times s$  CountSketch matrix and  $s < d_{\text{in}}$ . Assume that the entries of  $\mathbf{W}_{\text{old}}$  are IID and that the entries of  $\mathbf{V}$  are also IID. Then*

$$\mathbb{E} \|\widehat{\Delta} \mathbf{V}^T - \Delta \mathbf{V}^T\|_F^2 = \Omega\left(\frac{d_{\text{in}}}{s}\right) \cdot \|\mathbf{W}_{\text{old}} \mathbf{V}^T\|_F^2.$$

Since the magnitude of  $\Delta$  is much smaller than  $\mathbf{W}$ , especially when  $\mathbf{W}$  is close to a stationary point,  $\|\mathbf{W} \mathbf{V}^T\|_F^2$  is typically greater than  $\|\Delta \mathbf{V}^T\|_F^2$ . Thus,  $\mathbb{E} \|\widehat{\Delta} \mathbf{V}^T - \Delta \mathbf{V}^T\|_F^2$  is typically bigger than  $\|\Delta \mathbf{V}^T\|_F^2$ , which implies that using  $\widehat{\Delta}$  is no better than all-zeros or random guessing.

<sup>4</sup>The columns of  $\mathbf{S}_{\text{old}}$  and  $\mathbf{S}_{\text{new}}$  are randomly permuted. Even if  $\widetilde{\Delta}$  is close to  $\Delta$ , after randomly permuting the columns of  $\mathbf{S}_{\text{old}}$  or  $\mathbf{S}_{\text{new}}$ ,  $\widetilde{\Delta}$  becomes entirely different.

<sup>5</sup>In machine learning,  $\Delta$  is the updating direction, e.g., gradient. The magnitude of gradient is much smaller than the model parameters  $\mathbf{W}$ , especially when  $\mathbf{W}$  is close to a stationary point.

<sup>6</sup>The conclusion applies also to neural networks because its first layer is such a linear model.



**Defending the gradient matching attack of [58].** The gradient matching attack of [58] can recover the victim’s original data based on the victim’s gradient,  $\Delta_i$ , and the model parameters,  $\mathbf{W}$ . Numerical optimization is used to find the data on which the evaluated gradient matches  $\Delta_i$ . To get  $\Delta_i$ , the attacker must know  $\Delta$ . Using DBCL, no client knows  $\Delta$ . A smart attacker may want to use  $\hat{\Delta}$  in lieu of  $\Delta$  because of its unbiasedness. We show in Theorem 3 that this approach does not work.

**Theorem 3.** *Let  $\mathbf{S}_{old}$  and  $\mathbf{S}_{new}$  be  $d_{in} \times s$  CountSketch matrices and  $s < d_{in}$ . Then*

$$\mathbb{E} \|\hat{\Delta} - \Delta\|_F^2 = \Omega\left(\frac{d_{in}}{s}\right) \cdot \left(\|\mathbf{W}_{old}\|_F^2 + \|\mathbf{W}_{new}\|_F^2\right).$$

Theorem 3 is a trivial consequence of Theorem 1. Since the magnitude of  $\Delta$  is typically smaller than  $\mathbf{W}$ , Theorem 3 guarantees that using  $\hat{\Delta}$  is no better than all-zeros or random guessing.

### 6.3 Understanding DBCL from Optimization Perspective

We give an explanation of DBCL from optimization perspective. Let us consider the generalized linear model:

$$\operatorname{argmin}_{\mathbf{w}} \left\{ f(\mathbf{w}) \triangleq \frac{1}{n} \sum_{j=1}^n \ell(\mathbf{x}_j^T \mathbf{w}, y_j) \right\}, \quad (4)$$

where  $(\mathbf{x}_1, y_1), \dots, (\mathbf{x}_n, y_n)$  are the training samples and  $\ell(\cdot, \cdot)$  is the loss function. If we apply sketching to a generalized linear model, then the training will be solving the following problem:

$$\operatorname{argmin}_{\mathbf{w}} \left\{ \tilde{f}(\mathbf{w}) \triangleq \mathbb{E}_{\mathbf{S}} \left[ \frac{1}{n} \sum_{j=1}^n \ell(\mathbf{x}_j^T \mathbf{S} \mathbf{S}^T \mathbf{w}, y_j) \right] \right\}. \quad (5)$$

Note that (5) is different from (4). If  $\mathbf{S}$  is a uniform sampling matrix, then (5) will be empirical risk minimization with dropout. Prior work [47] proved that dropout is equivalent to adaptive regularization which can alleviate overfitting. Random projections such as CountSketch have the same properties as uniform sampling [51], and thus the role of random sketching in (5) can be thought of as adaptive regularization. This is why DBCL does not hinder prediction accuracy at all.

## 7 Related Work

Cryptography approaches such as secure aggregation [5], homomorphic encryption [1, 15, 16, 28, 56], Yao’s garbled circuit protocol [38], and many other methods [53, 55] can also improve the security of collaborative learning. Generative models such as [7, 46] can also improve privacy; however, they hinder the accuracy and efficiency, and their tuning and deployment are nontrivial. All the mentioned defenses are not competitive methods of our DBCL; instead, they can be combined with DBCL to defend more attacks.

Our methodology is based on matrix sketching [20, 11, 17, 30, 51, 10]. Sketching has been applied to achieve differential privacy [4, 21]. It has been shown that to protect privacy, matrix sketching has the same effect as injecting random noise. The contemporaneous work [25] applies sketching to federated learning for the sake of differential privacy. In particular, they apply the sketching to the gradients which are communicated between clients and server. Note the difference between [25] and our work: they directly sketch the gradients, whereas we sketch the model parameters. The two approaches look similar, however, the outcome is very different. Their method substantially hurts test accuracy, whereas our method does not hurt the accuracy at all.

Our method is developed based on the connection between sketching [51] and dropout training [42]; in particular, if  $\mathbf{S}$  is uniform sampling, then DBCL is essentially dropout. Our approach is different from [18] which directly applies matrix sketching to the gradients; DBCL, as well as dropout, applies matrix sketching to the model parameters. Our approach is similar to the contemporaneous work [22] which is developed for computational benefits.

Decentralized learning, that is, the clients perform peer-to-peer communication without a central server, is an alternative to federated learning and has received much attention in recent years [9, 23, 24, 29, 37, 40, 44, 49, 54]. The attacks of [33, 58] can be applied to decentralized learning, and DBCL can defend the attacks under the decentralized setting. We discuss decentralized learning in the appendix. The attacks and defense under the decentralized setting will be our future work.

## 8 Conclusions

Collaborative learning enables multiple parties to jointly train a model without data sharing. Unfortunately, standard distributed optimization algorithms can easily leak participants' privacy. We proposed Double-Blind Collaborative Learning (DBCL) for defending gradient-based attacks which are the most effective privacy inference methods. We showed that DBCL can defeat gradient-based attacks conducted by malicious clients. Admittedly, DBCL can not defend all kinds of attacks; for example, if the server is malicious, then the attack of [33] still works, but much less effectively. While it improves privacy, DBCL does not hurt test accuracy at all and does not much increase the cost of training. DBCL is easy to use and does not need extra tuning. Our future work will combine DBCL with cryptographic methods such as homomorphic encryption and secret sharing so that neither client nor server can infer users' privacy.

## Acknowledgments

The author thanks Giuseppe Ateniese, Danilo Francati, Michael Mahoney, Richard Peng, Peter Ríchtárik, and David Woodruff for their helpful suggestions.

## References

- [1] Yoshinori Aono, Takuya Hayashi, Lihua Wang, Shiho Moriai, et al. Privacy-preserving deep learning via additively homomorphic encryption. *IEEE Transactions on Information Forensics and Security*, 13(5):1333–1345, 2017.
- [2] Giuseppe Ateniese, Luigi V. Mancini, Angelo Spognardi, Antonio Villani, Domenico Vitali, and Giovanni Felici. Hacking smart machines with smarter ones: How to extract meaningful data from machine learning classifiers. *International Journal of Security and Networks*, 10(3):137–150, September 2015.
- [3] Pascal Bianchi, Gersende Fort, and Walid Hachem. Performance of a distributed stochastic approximation algorithm. *IEEE Transactions on Information Theory*, 59(11):7405–7418, 2013.
- [4] Jeremiah Blocki, Avrim Blum, Anupam Datta, and Or Sheffet. The Johnson-Lindenstrauss transform itself preserves differential privacy. In *Annual Symposium on Foundations of Computer Science (FOCS)*, 2012.
- [5] Keith Bonawitz, Vladimir Ivanov, Ben Kreuter, Antonio Marcedone, H Brendan McMahan, Sarvar Patel, Daniel Ramage, Aaron Segal, and Karn Seth. Practical secure aggregation for privacy preserving machine learning. *IACR Cryptology ePrint Archive*, 2017:281, 2017.
- [6] Moses Charikar, Kevin Chen, and Martin Farach-Colton. Finding frequent items in data streams. *Theoretical Computer Science*, 312(1):3–15, 2004.
- [7] Qingrong Chen, Chong Xiang, Minhui Xue, Bo Li, Nikita Borisov, Dali Kaarfar, and Haojin Zhu. Differentially private data generative models. *arXiv preprint arXiv:1812.02274*, 2018.
- [8] Kenneth L. Clarkson and David P. Woodruff. Low rank approximation and regression in input sparsity time. In *Annual ACM Symposium on theory of computing (STOC)*, 2013.
- [9] Igor Colin, Aurélien Bellet, Joseph Salmon, and Stéphan Clémencecon. Gossip dual averaging for decentralized optimization of pairwise functions. *arXiv preprint arXiv:1606.02421*, 2016.
- [10] Petros Drineas and Michael W Mahoney. RandNLA: randomized numerical linear algebra. *Communications of the ACM*, 59(6):80–90, 2016.
- [11] Petros Drineas, Michael W. Mahoney, and S. Muthukrishnan. Relative-error CUR matrix decompositions. *SIAM Journal on Matrix Analysis and Applications*, 30(2):844–881, September 2008.
- [12] Cynthia Dwork. Differential privacy. *Encyclopedia of Cryptography and Security*, pages 338–340, 2011.
- [13] Cynthia Dwork and Moni Naor. On the difficulties of disclosure prevention in statistical databases or the case for differential privacy. *Journal of Privacy and Confidentiality*, 2(1), 2010.

- [14] Matt Fredrikson, Somesh Jha, and Thomas Ristenpart. Model inversion attacks that exploit confidence information and basic countermeasures. In *Proceedings of the 22nd ACM SIGSAC Conference on Computer and Communications Security*, 2015.
- [15] Irene Giacomelli, Somesh Jha, Marc Joye, C David Page, and Kyonghwan Yoon. Privacy-preserving ridge regression with only linearly-homomorphic encryption. In *International Conference on Applied Cryptography and Network Security*, pages 243–261. Springer, 2018.
- [16] Ran Gilad-Bachrach, Nathan Dowlin, Kim Laine, Kristin Lauter, Michael Naehrig, and John Wernsing. CryptoNets: Applying neural networks to encrypted data with high throughput and accuracy. In *International Conference on Machine Learning (ICML)*, 2016.
- [17] Nathan Halko, Per-Gunnar Martinsson, and Joel A. Tropp. Finding structure with randomness: Probabilistic algorithms for constructing approximate matrix decompositions. *SIAM Review*, 53(2):217–288, 2011.
- [18] Filip Hanzely, Konstantin Mishchenko, and Peter Richtárik. SEGA: Variance reduction via gradient sketching. In *Advances in Neural Information Processing Systems (NeurIPS)*, 2018.
- [19] Briland Hitaj, Giuseppe Ateniese, and Fernando Perez-Cruz. Deep models under the GAN: information leakage from collaborative deep learning. In *Proceedings of the 2017 ACM SIGSAC Conference on Computer and Communications Security*, 2017.
- [20] William B. Johnson and Joram Lindenstrauss. Extensions of Lipschitz mappings into a Hilbert space. *Contemporary mathematics*, 26(189-206), 1984.
- [21] Krishnamurthy Kenthapadi, Aleksandra Korolova, Ilya Mironov, and Nina Mishra. Privacy via the Johnson-Lindenstrauss transform. *arXiv preprint arXiv:1204.2606*, 2012.
- [22] Ahmed Khaled and Peter Richtárik. Gradient descent with compressed iterates. *arXiv*, 2019.
- [23] Anastasia Koloskova, Sebastian U Stich, and Martin Jaggi. Decentralized stochastic optimization and gossip algorithms with compressed communication. *arXiv preprint arXiv:1902.00340*, 2019.
- [24] Guanghui Lan, Soomin Lee, and Yi Zhou. Communication-efficient algorithms for decentralized and stochastic optimization. *Mathematical Programming*, pages 1–48, 2017.
- [25] Tian Li, Zaoxing Liu, Vyas Sekar, and Virginia Smith. Privacy for free: Communication-efficient learning with differential privacy using sketches. *arXiv preprint arXiv:1911.00972*, 2019.
- [26] Xiang Li, Kaixuan Huang, Wenhao Yang, Shusen Wang, and Zhihua Zhang. On the convergence of FedAvg on Non-IID data. *arXiv:1907.02189*, 2019.
- [27] Xiangru Lian, Ce Zhang, Huan Zhang, Cho-Jui Hsieh, Wei Zhang, and Ji Liu. Can decentralized algorithms outperform centralized algorithms? a case study for decentralized parallel stochastic gradient descent. In *Advances in Neural Information Processing Systems (NIPS)*, 2017.
- [28] Yang Liu, Tianjian Chen, and Qiang Yang. Secure federated transfer learning. *arXiv preprint arXiv:1812.03337*, 2018.
- [29] Qinyi Luo, Jiaao He, Youwei Zhuo, and Xuehai Qian. Heterogeneity-aware asynchronous decentralized training. *arXiv preprint arXiv:1909.08029*, 2019.
- [30] Michael W. Mahoney. Randomized algorithms for matrices and data. *Foundations and Trends in Machine Learning*, 3(2):123–224, 2011.
- [31] Per-Gunnar Martinsson and Joel Tropp. Randomized numerical linear algebra: Foundations & algorithms. *arXiv preprint arXiv:2002.01387*, 2020.
- [32] Brendan McMahan, Eider Moore, Daniel Ramage, Seth Hampson, and Blaise Aguerre y Arcas. Communication-efficient learning of deep networks from decentralized data. In *Artificial Intelligence and Statistics (AISTATS)*, 2017.
- [33] Luca Melis, Congzheng Song, Emiliano De Cristofaro, and Vitaly Shmatikov. Exploiting unintended feature leakage in collaborative learning. In *IEEE Symposium on Security and Privacy (SP)*, 2019.
- [34] Xiangrui Meng and Michael W. Mahoney. Low-Distortion Subspace Embeddings in Input-Sparsity Time and Applications to Robust Linear Regression. In *Annual ACM Symposium on Theory of Computing (STOC)*, 2013.

- [35] John Nelson and Huy L. Nguyễn. OSNAP: Faster Numerical Linear Algebra Algorithms via Sparser Subspace Embeddings. In *IEEE Annual Symposium on Foundations of Computer Science (FOCS)*, 2013.
- [36] Ninh Pham and Rasmus Pagh. Fast and scalable polynomial kernels via explicit feature maps. In *ACM SIGKDD International Conference on Knowledge Discovery and Data Mining (KDD)*, 2013.
- [37] S Sundhar Ram, Angelia Nedić, and Venu V Veeravalli. Asynchronous gossip algorithm for stochastic optimization: Constant stepsize analysis. In *Recent Advances in Optimization and its Applications in Engineering*, pages 51–60. Springer, 2010.
- [38] Bitar Darvish Rouhani, M Sadegh Riazi, and Farinaz Koushanfar. DeepSecure: Scalable provably-secure deep learning. In *Proceedings of the 55th Annual Design Automation Conference*, 2018.
- [39] Anit Kumar Sahu, Tian Li, Maziar Sanjabi, Manzil Zaheer, Ameet Talwalkar, and Virginia Smith. Federated optimization for heterogeneous networks. *arXiv preprint arXiv:1812.06127*, 2019.
- [40] Benjamin Sirb and Xiaojing Ye. Consensus optimization with delayed and stochastic gradients on decentralized networks. In *2016 IEEE International Conference on Big Data (Big Data)*, pages 76–85. IEEE, 2016.
- [41] Kunal Srivastava and Angelia Nedic. Distributed asynchronous constrained stochastic optimization. *IEEE Journal of Selected Topics in Signal Processing*, 5(4):772–790, 2011.
- [42] Nitish Srivastava, Geoffrey Hinton, Alex Krizhevsky, Ilya Sutskever, and Ruslan Salakhutdinov. Dropout: a simple way to prevent neural networks from overfitting. *Journal of Machine Learning Research*, 15(1):1929–1958, 2014.
- [43] Sebastian U Stich. Local SGD converges fast and communicates little. *arXiv preprint arXiv:1805.09767*, 2018.
- [44] Hanlin Tang, Xiangru Lian, Ming Yan, Ce Zhang, and Ji Liu. D2: Decentralized training over decentralized data. *arXiv preprint arXiv:1803.07068*, 2018.
- [45] Mikkel Thorup and Yin Zhang. Tabulation-based 5-independent hashing with applications to linear probing and second moment estimation. *SIAM Journal on Computing*, 41(2):293–331, April 2012.
- [46] Aleksei Triastcyn and Boi Faltings. Federated generative privacy. *EPFL Tech. Report*, 2019.
- [47] Stefan Wager, Sida Wang, and Percy S Liang. Dropout training as adaptive regularization. In *Advances in Neural Information Processing Systems (NIPS)*, 2013.
- [48] Jianyu Wang and Gauri Joshi. Cooperative SGD: A unified framework for the design and analysis of communication-efficient SGD algorithms. *arXiv preprint arXiv:1808.07576*, 2018.
- [49] Jianyu Wang, Anit Kumar Sahu, Zhouyi Yang, Gauri Joshi, and Soumya Kar. Matcha: Speeding up decentralized sgd via matching decomposition sampling. *arXiv preprint arXiv:1905.09435*, 2019.
- [50] Kilian Weinberger, Anirban Dasgupta, John Langford, Alex Smola, and Josh Attenberg. Feature hashing for large scale multitask learning. In *International Conference on Machine Learning (ICML)*, 2009.
- [51] David P Woodruff. Sketching as a tool for numerical linear algebra. *Foundations and Trends® in Theoretical Computer Science*, 10(1–2):1–157, 2014.
- [52] Hao Yu, Sen Yang, and Shenghuo Zhu. Parallel restarted sgd with faster convergence and less communication: Demystifying why model averaging works for deep learning. In *AAAI Conference on Artificial Intelligence*, 2019.
- [53] Jiawei Yuan and Shucheng Yu. Privacy preserving back-propagation neural network learning made practical with cloud computing. *IEEE Transactions on Parallel and Distributed Systems*, 25(1):212–221, 2013.
- [54] Kun Yuan, Qing Ling, and Wotao Yin. On the convergence of decentralized gradient descent. *SIAM Journal on Optimization*, 26(3):1835–1854, 2016.

- [55] Dayin Zhang, Xiaojun Chen, Dakui Wang, and Jinqiao Shi. A survey on collaborative deep learning and privacy-preserving. In *IEEE Third International Conference on Data Science in Cyberspace (DSC)*, 2018.
- [56] Qiao Zhang, Cong Wang, Hongyi Wu, Chunsheng Xin, and Tran V Phuong. GELU-Net: A globally encrypted, locally unencrypted deep neural network for privacy-preserved learning. In *International Joint Conferences on Artificial Intelligence (IJCAI)*, 2018.
- [57] Fan Zhou and Guojing Cong. On the convergence properties of a k-step averaging stochastic gradient descent algorithm for nonconvex optimization. *arXiv preprint arXiv:1708.01012*, 2017.
- [58] Ligeng Zhu, Zhijian Liu, and Song Han. Deep leakage from gradients. In *Advances in Neural Information Processing Systems (NeurIPS)*, 2019.

## A Algorithm Derivation

In this section, we derive the algorithm outlined in Section 4. In Section A.1 and A.2, we apply sketching to dense layer and convolutional layer, respectively, and derive the gradients.

### A.1 Dense Layers

For simplicity, we study the case of batch size  $b = 1$  for a dense layer. Let  $\mathbf{x} \in \mathbb{R}^{1 \times d_{\text{in}}}$  be the input,  $\mathbf{W} \in \mathbb{R}^{d_{\text{out}} \times d_{\text{in}}}$  be the parameter matrix,  $\mathbf{S} \in \mathbb{R}^{d_{\text{in}} \times s}$  ( $s < d_{\text{in}}$ ) be a sketching matrix, and

$$\mathbf{z} = \mathbf{xS}(\mathbf{WS})^T \in \mathbb{R}^{1 \times d_{\text{out}}}$$

be the output (during training). For out-of-sample prediction, sketching is not applied, equivalently,  $\mathbf{S} = \mathbf{I}_{d_{\text{in}}}$ .

In the following, we describe how to propagate gradient from the loss function back to  $x$  and  $\mathbf{W}$ . The dependence among the variables can be depicted as

$$\text{input} \longrightarrow \cdots \longrightarrow \underbrace{\left. \begin{array}{c} \mathbf{x} \\ \mathbf{W} \end{array} \right\}}_{\text{the studied layer}} \longrightarrow \mathbf{z} \longrightarrow \cdots \longrightarrow \text{loss.}$$

During the backpropagation, the gradients propagated to the studied layer are

$$\mathbf{g} \triangleq \frac{\partial L}{\partial \mathbf{z}} \in \mathbb{R}^{1 \times d_{\text{out}}}, \quad (6)$$

where  $L$  is some loss function. Then we further propagate the gradient from  $\mathbf{z}$  to  $\mathbf{x}$  and  $\mathbf{W}$ :

$$\frac{\partial L}{\partial \mathbf{x}} = \frac{\partial L}{\partial \mathbf{z}} \frac{\partial \mathbf{z}}{\partial (\mathbf{xS})} \frac{\partial (\mathbf{xS})}{\partial \mathbf{x}} = \mathbf{g}(\mathbf{WS})\mathbf{S}^T \in \mathbb{R}^{1 \times d_{\text{in}}}, \quad (7)$$

$$\frac{\partial L}{\partial \mathbf{W}} = \mathbf{g}^T(\mathbf{xS})\mathbf{S}^T \in \mathbb{R}^{d_{\text{out}} \times d_{\text{in}}}. \quad (8)$$

We prove (8) in the following. Let  $\tilde{\mathbf{x}} = \mathbf{xS} \in \mathbb{R}^{1 \times s}$  and  $\tilde{\mathbf{W}} = \mathbf{WS} \in \mathbb{R}^{d_{\text{out}} \times s}$ . Let  $\mathbf{w}_j$ ; and  $\tilde{\mathbf{w}}_j$ ; be the  $j$ -th row of  $\mathbf{W}$  and  $\tilde{\mathbf{W}}$ , respectively. It can be shown that

$$\frac{\partial L}{\partial \tilde{\mathbf{w}}_j} = \sum_{l=1}^{d_{\text{out}}} \frac{\partial L}{\partial z_l} \frac{\partial z_l}{\partial \tilde{\mathbf{w}}_j} = \sum_{l=1}^{d_{\text{out}}} \frac{\partial L}{\partial z_l} \frac{\partial (\tilde{\mathbf{x}}\tilde{\mathbf{w}}_l^T)}{\partial \tilde{\mathbf{w}}_j} = \frac{\partial L}{\partial z_j} \frac{\partial (\tilde{\mathbf{x}}\tilde{\mathbf{w}}_j^T)}{\partial \tilde{\mathbf{w}}_j} = g_j \tilde{\mathbf{x}} \in \mathbb{R}^{1 \times s}.$$

Thus,  $\tilde{\mathbf{w}}_j = \mathbf{w}_j\mathbf{S} \in \mathbb{R}^{1 \times s}$ ; moreover,  $\tilde{\mathbf{w}}_j$ ; is independent of  $\mathbf{w}_l$ ; if  $j \neq l$ . It follows that

$$\frac{\partial L}{\partial \mathbf{w}_j} = \frac{\partial L}{\partial \tilde{\mathbf{w}}_j} \frac{\partial \tilde{\mathbf{w}}_j}{\partial \mathbf{w}_j} = g_j \tilde{\mathbf{x}}\mathbf{S}^T \in \mathbb{R}^{1 \times d_{\text{in}}}.$$

Thus

$$\frac{\partial L}{\partial \mathbf{W}} = \mathbf{g}^T \tilde{\mathbf{x}}\mathbf{S}^T = \mathbf{g}^T(\mathbf{xS})\mathbf{S}^T \in \mathbb{R}^{d_{\text{out}} \times d_{\text{in}}}.$$

### A.2 Extension to Convolutional Layers

Let  $\mathbf{X}$  be a  $d_1 \times d_2 \times d_3$  tensor and  $\mathbf{K}$  be a  $k_1 \times k_2 \times d_3$  kernel. The convolution  $\mathbf{X} * \mathbf{K}$  outputs a  $d_1 \times d_2$  matrix (assume zero-padding is used). The convolution can be equivalently written as matrix-vector multiplication in the following way.

We segment  $\mathbf{X}$  to many patches of shape  $k_1 \times k_2 \times d_3$  and then reshape every patch to a  $d_{\text{in}} \triangleq k_1 k_2 d_3$ -dimensional vector. Let  $\mathbf{p}_i$  be the  $i$ -th patch (vector). Tensor  $\mathbf{X}$  has  $q \triangleq d_1 d_2$  such patches. Let

$$\mathbf{P} \triangleq [\mathbf{p}_1, \dots, \mathbf{p}_q]^T \in \mathbb{R}^{q \times d_{\text{in}}}$$

be the concatenation of the patches. Let  $\mathbf{w} \in \mathbb{R}^{d_{\text{in}}}$  be the vectorization of the kernel  $\mathbf{K} \in \mathbb{R}^{k_1 \times k_2 \times d_3}$ . The matrix-vector product,  $\mathbf{z} = \mathbf{Pw} \in \mathbb{R}^q$ , is indeed the vectorization of the convolution  $\mathbf{X} * \mathbf{K}$ .

In practice, we typically use multiple kernels for the convolution; let  $\mathbf{W} \triangleq [\mathbf{w}_1, \dots, \mathbf{w}_{d_{\text{out}}}]^T \in \mathbb{R}^{d_{\text{out}} \times d_{\text{in}}}$  be the concatenation of  $d_{\text{out}}$  different (vectorized) kernels. In this way, the convolution of  $\mathbf{X}$  with  $d_{\text{out}}$  different kernels, which outputs a  $d_1 \times d_2 \times r$  tensor, is the reshape of  $\mathbf{X}\mathbf{W}^T \in \mathbb{R}^{q \times d_{\text{out}}}$ .

We show in the above that tensor convolution can be equivalently expressed as matrix-matrix multiplication. Therefore, we can apply matrix sketching to convolutional layers in the same way as the dense layer. Specifically, let  $\mathbf{S}$  be a  $d_{\text{in}} \times s$  random sketching matrix. Then  $\mathbf{X}\mathbf{S}(\mathbf{W}\mathbf{S})^T$  is an approximation to  $\mathbf{X}\mathbf{W}^T$ , and the backpropagation is accordingly derived using matrix differentiation.

## B Proofs

In this section, we prove Theorem 1 and Corollary 2. Theorem 1 follows from Lemmas 4 and 5. Corollary 2 follows from Lemma 6.

**Lemma 4.** *Let  $\mathbf{S}_{\text{old}}$  and  $\mathbf{S}_{\text{new}}$  be independent CountSketch matrices. For any matrix  $\mathbf{V}$  independent of  $\mathbf{S}_{\text{old}}$  and  $\mathbf{S}_{\text{new}}$ , the following identity holds:*

$$\begin{aligned} & \mathbb{E} \left\| \widehat{\Delta} \mathbf{V}^T - \Delta \mathbf{V}^T \right\|_F^2 \\ &= \mathbb{E} \left\| \mathbf{W}_{\text{old}} \mathbf{V}^T - \mathbf{W}_{\text{old}} \mathbf{S}_{\text{old}} \mathbf{S}_{\text{old}}^T \mathbf{V}^T \right\|_F^2 + \mathbb{E} \left\| \mathbf{W}_{\text{new}} \mathbf{V}^T - \mathbf{W}_{\text{new}} \mathbf{S}_{\text{new}} \mathbf{S}_{\text{new}}^T \mathbf{V}^T \right\|_F^2, \end{aligned}$$

where the expectation is taken w.r.t. the random sketching matrices  $\mathbf{S}_{\text{old}}$  and  $\mathbf{S}_{\text{new}}$ .

*Proof.* Recall the definitions:  $\Delta = \mathbf{W}_{\text{old}} - \mathbf{W}_{\text{new}}$  and  $\widehat{\Delta} = \mathbf{W}_{\text{old}} \mathbf{S}_{\text{old}} \mathbf{S}_{\text{old}}^T - \mathbf{W}_{\text{new}} \mathbf{S}_{\text{new}} \mathbf{S}_{\text{new}}^T$ . Then

$$\begin{aligned} \left\| \widehat{\Delta} \mathbf{V}^T - \Delta \mathbf{V}^T \right\|_F^2 &= \left\| (\mathbf{W}_{\text{old}} \mathbf{S}_{\text{old}} \mathbf{S}_{\text{old}}^T - \mathbf{W}_{\text{new}} \mathbf{S}_{\text{new}} \mathbf{S}_{\text{new}}^T) \mathbf{V}^T - \Delta \mathbf{V}^T \right\|_F^2 \\ &= \left\| (\mathbf{W}_{\text{old}} \mathbf{S}_{\text{old}} \mathbf{S}_{\text{old}}^T - \mathbf{W}_{\text{new}} \mathbf{S}_{\text{new}} \mathbf{S}_{\text{new}}^T) \mathbf{V}^T - (\mathbf{W}_{\text{old}} - \mathbf{W}_{\text{new}}) \mathbf{V}^T \right\|_F^2 \\ &= \left\| \mathbf{W}_{\text{old}} (\mathbf{S}_{\text{old}} \mathbf{S}_{\text{old}}^T - \mathbf{I}) \mathbf{V}^T + \mathbf{W}_{\text{new}} (\mathbf{I} - \mathbf{S}_{\text{new}} \mathbf{S}_{\text{new}}^T) \mathbf{V}^T \right\|_F^2 \\ &= \left\| \mathbf{W}_{\text{old}} (\mathbf{S}_{\text{old}} \mathbf{S}_{\text{old}}^T - \mathbf{I}) \mathbf{V}^T \right\|_F^2 + \left\| \mathbf{W}_{\text{new}} (\mathbf{I} - \mathbf{S}_{\text{new}} \mathbf{S}_{\text{new}}^T) \mathbf{V}^T \right\|_F^2 \\ &\quad + 2 \left\langle \mathbf{W}_{\text{old}} (\mathbf{S}_{\text{old}} \mathbf{S}_{\text{old}}^T - \mathbf{I}) \mathbf{V}^T, \mathbf{W}_{\text{new}} (\mathbf{I} - \mathbf{S}_{\text{new}} \mathbf{S}_{\text{new}}^T) \mathbf{V}^T \right\rangle. \end{aligned}$$

Since  $\mathbb{E}[\mathbf{S}_{\text{old}} \mathbf{S}_{\text{old}}^T - \mathbf{I}] = \mathbf{0}$ ,  $\mathbb{E}[\mathbf{S}_{\text{new}} \mathbf{S}_{\text{new}}^T - \mathbf{I}] = \mathbf{0}$ , and  $\mathbf{S}_{\text{old}}$  and  $\mathbf{S}_{\text{new}}$  are independent, we have

$$\mathbb{E} \left[ \left\langle \mathbf{W}_{\text{old}} (\mathbf{S}_{\text{old}} \mathbf{S}_{\text{old}}^T - \mathbf{I}) \mathbf{V}^T, \mathbf{W}_{\text{new}} (\mathbf{I} - \mathbf{S}_{\text{new}} \mathbf{S}_{\text{new}}^T) \mathbf{V}^T \right\rangle \right] = 0.$$

It follows that

$$\begin{aligned} & \mathbb{E} \left\| \widehat{\Delta} \mathbf{V}^T - \Delta \mathbf{V}^T \right\|_F^2 \\ &= \mathbb{E} \left\| \mathbf{W}_{\text{old}} (\mathbf{S}_{\text{old}} \mathbf{S}_{\text{old}}^T - \mathbf{I}) \mathbf{V}^T \right\|_F^2 + \mathbb{E} \left\| \mathbf{W}_{\text{new}} (\mathbf{I} - \mathbf{S}_{\text{new}} \mathbf{S}_{\text{new}}^T) \mathbf{V}^T \right\|_F^2, \end{aligned}$$

by which the lemma follows.  $\square$

**Lemma 5.** *Let  $\mathbf{S}$  be a  $d \times s$  CountSketch matrix. Let  $\mathbf{A} \in \mathbb{R}^{n \times d}$  and  $\mathbf{B} \in \mathbb{R}^{m \times d}$  be any non-random matrices. Then*

$$\mathbb{E} [\mathbf{A} \mathbf{S} \mathbf{S}^T \mathbf{B}^T - \mathbf{A} \mathbf{B}^T]^2 = \frac{1}{s} \sum_{i=1}^n \sum_{j=1}^m \left( \sum_{k \neq l} a_{ki}^2 b_{lj}^2 + \sum_{k \neq l} a_{ki} b_{kj} a_{li} b_{lj} \right).$$

*Proof.* [36, 50] showed that for any vectors  $\mathbf{a}, \mathbf{b} \in \mathbb{R}^d$ ,

$$\begin{aligned} \mathbb{E} [\mathbf{a}^T \mathbf{S} \mathbf{S}^T \mathbf{b}] &= \mathbf{a}^T \mathbf{b}, \\ \mathbb{E} [\mathbf{a}^T \mathbf{S} \mathbf{S}^T \mathbf{b} - \mathbf{a}^T \mathbf{b}]^2 &= \frac{1}{s} \left( \sum_{k \neq l} a_k^2 b_l^2 + \sum_{k \neq l} a_k b_k a_l b_l \right). \end{aligned}$$

Let  $\mathbf{a}_i \in \mathbb{R}^d$  be the  $i$ -th row of  $\mathbf{A} \in \mathbb{R}^{n \times d}$  and  $\mathbf{b}_j \in \mathbb{R}^d$  be the  $j$ -th column of  $\mathbf{B} \in \mathbb{R}^{m \times d}$ . Then,

$$\begin{aligned} \mathbb{E}[\mathbf{A}\mathbf{S}\mathbf{S}^T\mathbf{B}^T - \mathbf{A}\mathbf{B}^T]^2 &= \sum_{i=1}^n \sum_{j=1}^m \mathbb{E}[\mathbf{a}_i^T \mathbf{S}\mathbf{S}^T \mathbf{b}_j - \mathbf{a}_i^T \mathbf{b}_j]^2 \\ &= \frac{1}{s} \sum_{i=1}^n \sum_{j=1}^m \left( \sum_{k \neq l} a_{ik}^2 b_{jl}^2 + \sum_{k \neq l} a_{ik} b_{jk} a_{il} b_{jl} \right), \end{aligned}$$

by which the lemma follows.  $\square$

**Lemma 6.** Let  $\mathbf{S}$  be a  $d \times s$  CountSketch matrix. Assume that the entries of  $\mathbf{A}$  are IID and that the entries of  $\mathbf{B}$  are also IID. Then

$$\mathbb{E}[\mathbf{A}^T \mathbf{S}\mathbf{S}^T \mathbf{B} - \mathbf{A}^T \mathbf{B}]^2 = \Theta\left(\frac{d}{s}\right) \|\mathbf{A}\mathbf{B}^T\|_F^2.$$

*Proof.* Assume all the entries of  $\mathbf{A}$  are IID sampled from a distribution with mean  $\mu_A$  and standard deviation  $\sigma_A$ ; assume all the entries of  $\mathbf{B}$  are IID sampled from a distribution with mean  $\mu_B$  and standard deviation  $\sigma_B$ . It follows from Lemma 5 that

$$\begin{aligned} \mathbb{E}[\mathbf{A}\mathbf{S}\mathbf{S}^T\mathbf{B}^T - \mathbf{A}\mathbf{B}^T]^2 &= \frac{mn}{s} [(d^2 - d)(\mu_A^2 + \sigma_A^2)(\mu_B^2 + \sigma_B^2) + (d^2 - d)\mu_A^2 \mu_B^2] \\ &= \Theta\left(\frac{mnd^2}{s} (\mu_A^2 + \sigma_A^2)(\mu_B^2 + \sigma_B^2)\right) = \Theta\left(\frac{d}{s}\right) \|\mathbf{A}\mathbf{B}^T\|_F^2. \end{aligned}$$

$\square$

## C Decentralized Learning

Instead of relying on a central server, multiple parties can collaborate using such a peer-to-peer network as Figure 5. A client is a compute node in the graph and connected to a few neighboring nodes. Many decentralized optimization algorithms have been developed [3, 54, 40, 9, 27, 24, 44]. The nodes collaborate by, for example, aggregating its neighbors' model parameters, taking a weighted average of neighbors' and its own parameters as the intermediate parameters, and then locally performing an SGD update.

We find that the attacks of [33, 58] can be applied to this kind of decentralized learning. Note that a node shares its model parameters with its neighbors. If a node is malicious, it can use its neighbors' gradients and model parameters to infer their data. Let a neighbor's (the victim) parameters in two consecutive rounds be  $\mathbf{W}_{\text{old}}$  and  $\mathbf{W}_{\text{new}}$ . The difference,  $\Delta = \mathbf{W}_{\text{old}} - \mathbf{W}_{\text{new}}$ , is mainly the gradient evaluated on the victim's data.<sup>7</sup> With the model parameters  $\mathbf{W}$  and updating direction  $\Delta$  at hand, the attacker can perform the gradient-based attacks of [33, 58].

Our DBCL can be easily applied under the decentralized setting: two neighboring compute nodes agree upon the random seeds, sketching their model parameters, and communicate the sketches. This can stop any node from knowing,  $\Delta = \mathbf{W}_{\text{old}} - \mathbf{W}_{\text{new}}$ , i.e., the gradient of the neighbor. We will empirically study the decentralized setting in our future work.

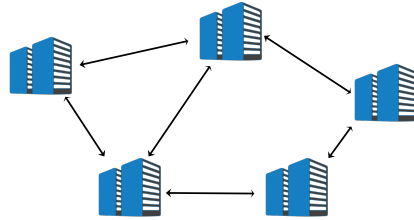


Figure 5: Decentralized learning in a peer-to-peer network.

<sup>7</sup>Besides the victim's gradient,  $\Delta$  contains the victim's neighbors' gradients, but their weights are usually lower than the victim's gradient.